Iron(III) Compounds

DOI: 10.1002/ange.200601774

A Square-Planar Organoiron(III) Compound with a Spin-Admixed State**

Pablo J. Alonso, Ana B. Arauzo, Juan Forniés, M. Angeles García-Monforte, Antonio Martín, Jesús I. Martínez, Babil Menjón,* Conrado Rillo, and José J. Sáiz-Garitaonandia*

Dedicated to Dr. Francisco Martínez-Buenaga on the occasion of his 60th birthday

Iron is an abundant, inexpensive, and essentially nontoxic element that is of central importance in almost every branch of chemistry, materials science and technology, and life

[*] Prof. Dr. P. J. Alonso, Prof. Dr. J. Forniés, Dr. M. A. García-Monforte, Dr. A. Martín, Dr. J. I. Martínez, Dr. B. Menjón, Prof. Dr. C. Rillo
Instituto de Ciencia de Materiales de Aragón
Universidad de Zaragoza and C.S.I.C.
C/Pedro Cerbuna 12, Zaragoza (Spain)
Fax: (+34) 976-761-187
E-mail: alonso@unizar.es
menjon@unizar.es

Dr. J. J. Sáiz-Garitaonandia
Departamento de Física Aplicada II
Facultad de Ciencia y Tecnología
Universidad del País Vasco
Apdo. 644, 48080 Bilbao (Spain)

Dr. A. B. Arauzo
Servicio de Instrumentación Científica, Medidas Físicas
Universidad de Zaragoza
C/Pedro Cerbuna 12, Zaragoza (Spain)

[**] This work was supported by the Spanish MCYT (DGI)/FEDER (projects CTQ2005-08606-C02-01 and BFU2005-07422-C02-02) and the Gobierno de Aragón (Grupo de Excelencia: Química Inorgánica y de los Compuestos Organometálicos). We are indebted to Prof. Dr. S. Alvarez (Universitat de Barcelona) for kindly providing values of continuous-shape measurements as well as for sharing results prior to publication.

Supporting information for this article (Experimental Section, the model developed to explain the physical properties of **1**, and additional Mössbauer and EPR spectra of **1**) is available on the WWW under http://www.angewandte.org or from the author.

© 2006 Wiley-VCH Verlag GmbH & Co. KGaA, Weinheim

science.[1,2] Much effort has been devoted to studying the magnetic properties of several classes of iron derivatives in different oxidation states (especially Fe^{II} and Fe^{III}) because of their relevance to various biological systems.[3] Underlying this intensive research is one of the ultimate goals in chemistry—to understand the relationship between electronic structure, molecular geometry, and as many chemical, magnetic, and spectroscopic properties as possible.[4] Fe^{III} is a d^5 ion that usually adopts tetrahedral (T-4) or octahedral (OC-6) environments when surrounded by four or six substituents, respectively.[1,5] Mononuclear Fe^{III} derivatives in both these coordination environments usually exhibit a high-spin (HS) configuration ($S = {}^5/_2$), and only in the OC-6 case is the action of strong-field ligands able to induce the electron-pairing that gives rise to the low-spin (LS) configuration ($S = {}^1/_2$). Interesting cases of spin crossover between the HS and LS configurations have also been described.[6] A particularly rich magnetic behavior has been observed in six- or five-coordinate Fe^{III} porphyrins, phthalocyanines, and related derivatives bearing macrocyclic ligands, be they synthetic or protein-bound: in addition to the common HS and LS configurations, examples of intermediate-spin ($S = {}^3/_2$), as well as spin-admixed (that is, mixed-spin, $S = {}^3/_2, {}^5/_2$) configurations have been reported.[7] Intermediate-spin states have also been found in square-pyramidal (SPY-5) Fe^{III} complexes.[8] In contrast to all these well-established coordination polyhedra, the square-planar (SP-4) geometry is virtually absent from Fe^{III} chemistry and, hence, little is known with certainty about the magnetic properties associated with the d^5 ion in this coordination environment. Herein, we report on the synthesis and characterization of an unambiguously established SP-4 Fe^{III} compound, as well as the study of its magnetic properties.

Anhydrous $FeCl_3$ was found to react with LiC_6Cl_5 in Et_2O to give the organometallic anion $[Fe^{III}(C_6Cl_5)_4]^-$, which was isolated in reasonable yield as the $[Li(thf)_4]^+$ salt (**1**, Scheme 1).[9] Compound **1** is an extremely rare example of a

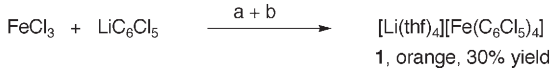

Scheme 1. Experimental procedure to obtain **1**: a) reaction in Et_2O at −78 °C; b) addition of THF.

homoleptic σ-organoiron(III) derivative for which the only precedent could possibly be the alkynyl complex $K_3[Fe^{III}(C{\equiv}CH)_6]$, which was obtained by oxidation of the precursor $K_4[Fe^{II}(C{\equiv}CH)_6]$ with O_2 in liquid ammonia.[10] Unfortunately, however, the high thermal instability of the oxidized alkynyl species, together with its proneness to explode, precluded even a minimally satisfactory characterization of the material. All other σ-organoiron(III) compounds invariably contain ancillary ligands, to enhance the stability of the corresponding organometallic species.[11]

The synthetic method leading to **1** is also noteworthy in that the Fe^{III} ion undergoes full arylation without undergoing any redox process. $FeCl_3$ and other simple Fe^{III} substrates are known to react with organolithium or -magnesium reagents to give organoiron(II) derivatives[12] or lower-valent species of mostly uncertain stoichiometries. Many of these reduced species show interesting reactivity patterns for application in organic synthesis.[13] The ability of $FeCl_3$ to promote C–C coupling reactions was noted very early on.[14] In this context, it is interesting to recall that one of the two original methods for the synthesis of ferrocene was, in fact, intended to give fulvalene by the $FeCl_3$-promoted reductive coupling of C_5H_5MgBr.[15] An exception to this reductive behavior is found in the reaction of $FeCl_3$ with norborn-1-yllithium, which has been reported to proceed with oxidation of the metal center to give $[Fe^{IV}(norborn\text{-}1\text{-}yl)_4]$.[16] It was suggested by the authors that *"negatively charged complexes probably form"* during this reaction, although these were not detected.

The crystal and molecular structure of **1** was established by single-crystal X-ray diffraction. There are two sets of crystallographically independent $[Li(thf)_4]^+$ and $[Fe^{III}(C_6Cl_5)_4]^-$ ions in the crystal lattice; since they show no significant differences, we will discuss only one of them. The Fe^{III} centers in the lattice are well separated from each other, with the smallest intermetallic distance being greater than 1.1 nm. The $[Li(thf)_4]^+$ ion shows the usual tetrahedral (T-4) arrangement of the thf molecules around the Li^+ ion.[17] The local coordination environment of the Fe^{III} center in the $[Fe^{III}(C_6Cl_5)_4]^-$ ion (Figure 1) can be described as slightly distorted SP-4, in light of the low value of the continuous-shape measure determined for that geometry (0.41 for SP-4 versus 27.96 for T-4).[18] The Fe^{III} ion lies in the best coordination plane (imposed by symmetry), while each pair of *trans*-oriented carbon atoms depart slightly from it in opposite directions (±12 pm), which results in an incipient tetrahedral distortion. The C_6Cl_5 rings are helicoidally arranged around the Fe^{III} center and form angles of 63.6 and 53.4° with the coordination plane. This helicoidal

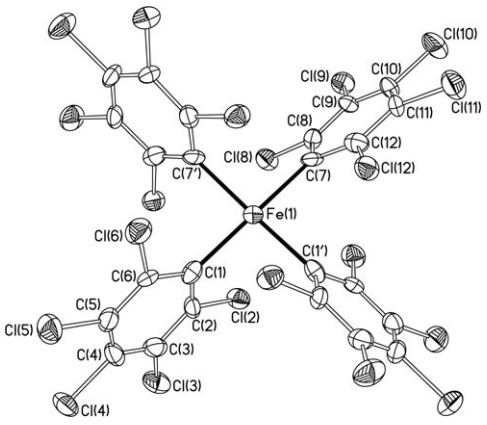

Figure 1. Thermal ellipsoid diagram (50% probability) of one of the two crystallographically independent $[Fe(C_6Cl_5)_4]^-$ ions in **1**. Selected bond lengths [pm] and angles [°] with estimated standard deviations: Fe(1)–C(1) 207.8(10), Fe(1)–C(7) 205.0(9); C(1)–Fe(1)–C(7) 173.2(4), C(1)–Fe(1)–C(1′) 93.5(5), C(1)–Fe(1)–C(7′) 87.5(4), C(7)–Fe(1)–C(7′) 92.2(5), C(2)–C(1)–Fe(1) 116.2(6), C(6)–C(1)–Fe(1) 128.2(7), C(8)–C(7)–Fe(1) 118.4(7), C(12)–C(7)–Fe(1) 126.8(7). Nonbonding distances to *ortho*-chlorine atoms [pm]: Fe(1)···Cl(2) 313.8, Fe(1)···Cl(6) 355.2, Fe(1)···Cl(8) 318.2, Fe(1)···Cl(12) 353.8. The smallest distance between iron centers is 1.109 nm, which corresponds to the Fe(1)···Fe(2) separation.

© 2006 Wiley-VCH Verlag GmbH & Co. KGaA, Weinheim

arrangement makes the whole anion chiral (the one depicted in Figure 1 is the clockwise (*C*) enantiomer). Moreover, the C_6Cl_5 groups also exhibit a considerable swing about the *ipso*-carbon atoms, which results in different Fe–C^{ipso}–C^{ortho} angles and different Fe···Cl^{ortho} distances within each ring. All the Fe···Cl^{ortho} distances are too long (> 310 pm) to be considered as indicative of any bonding interaction. Moreover, in those cases in which such M···Cl^{ortho} secondary bonding interactions do occur, very distorted coordination polyhedra are observed because of the high strain associated with the small-bite chelating ligand C_6Cl_5-$\kappa C,\kappa^2 Cl$ (compare to the pseudo-octahedral structure found for the isoleptic d^3 species $[Cr^{III}(C_6Cl_5)_4]^-$).[17] The distortions found in the environment of the Fe^{III} center in **1** involve a decrease in the effective symmetry from the ideal D_{4h} to approximately D_2 symmetry.

There has been much interest in obtaining four-coordinate Fe^{III} derivatives with SP-4 geometry, especially those containing macrocyclic-$\kappa^4 N$ ligands because of their relevance to heme systems. That geometry, however, has proven to be highly elusive in Fe^{III} chemistry, since additional axial interactions are generally established that eventually yield five- or six-coordinate species.[7] Even so-called weakly coordinating ligands become involved in such axial interactions. For instance, axial agostic interactions have been suggested to be present between the Fe^{III} center and the remote methyl substituents of the porphyrinogen ring in $[Li(NCMe)_4][Fe^{III}\{LMe_8\text{-}\kappa^4 N\}]$ (H_4LMe_8 = *meso*-octamethylporphyrinogen).[19] The closely related species $[NEt_4][Fe^{III}\{LCy_4\text{-}\kappa^4 N\}]$ (H_4LCy_4 = *meso*-tetracyclohexylporphyrinogen) has also been reported recently, but has not yet been described in detail.[20] The magnetic properties of all these species depend strongly on the relative strengths of the equatorial versus axial iron–ligand bonding interactions. Based on this dependence, a new scale for the σ-donor ability of a ligand has been derived recently: the magnetochemical series.[21] Considering the formal relationship between the aromatic *C*-donor phenyl and *N*-donor pyrrolyl rings, complex **1** can be considered as a model for Fe^{III} heme systems with no axial ligands.[22] Hence, a physical characterization of **1**, including a detailed study of its magnetic behavior, seemed to be of interest.

The ^{57}Fe Mössbauer spectrum of **1** at 77 K is shown in Figure 2a. The dominant contribution[23] is a doublet with an isomer shift of $\delta = 0.20(1)\ mm\,s^{-1}$ and a quadrupolar splitting of $\Delta E_Q = 3.00(1)\ mm\,s^{-1}$, typical of an Fe^{III} entity in an $S = {}^3/_2$ or a spin-admixed state. Spectral features with similar δ and ΔE_Q values are observed for **1** in the temperature range of 14–200 K. Asymmetric broadening of the quadrupolar-doublet components appears at temperatures below 77 K (see Supporting Information for the Mössbauer spectrum of **1** at 14 K).

The X- (Figure 2b) and Q-band (see Supporting Information) EPR spectra of **1** at 10 K can be ascribed to a paramagnetic entity with an effective spin of $S' = {}^1/_2$ and a markedly orthorhombic effective *g* tensor (*g*′) with the principal values given in Table 1. This spectrum is qualitatively similar to that reported for the five-coordinate $S = {}^3/_2$ species $[Fe^{III}\{LR_2R'_2\text{-}\kappa^4 N\}I]$, where $\{LR_2R'_2\}^{2-}$ is the 6,13-bis(ethoxycarbonyl)-5,14-dimethyl-1,4,8,11-tetraazacyclotetradeca-4,6,12,14-tetraenato(2−) ligand.[24] When the temperature is increased, the EPR spectra of **1** broaden and their intensities decrease sharply, becoming undetectable at temperatures above 40 K (see Supporting Information).

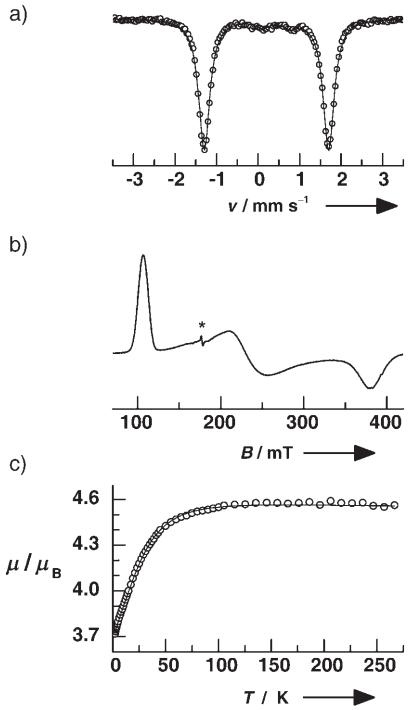

Figure 2. Physical properties of **1** (polycrystalline samples). a) ^{57}Fe Mössbauer spectrum recorded at 77 K in the absence of a magnetic field.[23] b) X-band EPR spectrum recorded at 10 K; the signal marked * at 170 mT is due to the cavity. c) Plot of the effective magnetic moment as a function of temperature; the solid line represents the calculated thermal evolution (see text).

The magnetic susceptibility (χ) of **1** was measured as a function of temperature in the range 1.8–265 K. After correcting for the temperature-independent contribution (χ_{TI}), the magnetic moment (μ) was deduced.[25] Its thermal evolution, $\mu(T)$, is depicted in Figure 2c, and the high- and low-temperature limit values (μ_∞ and μ_0) are given in Table 1.

Table 1: Experimental and calculated parameters associated with the magnetic properties of **1**.

Parameter	Experimental	Calculated
g'_x	2.98(2)	3.01(1)
g'_y	6.52(2)	6.51(1)
g'_z	1.84(2)	1.71(1)
μ_0/μ_B	3.7(1)	3.67(2)
μ_∞/μ_B	4.6(1)	4.52(2)

A value of $\mu_\infty \approx 3.9\ \mu_B$ is expected for a pure intermediate-spin Fe^{III} species with an orbital singlet ground-state. The higher value obtained for **1** ($\mu_\infty = 4.6(1)\ \mu_B$) can be explained by considering a spin-admixed ($S = {}^3/_2, {}^5/_2$) state. These types of systems have been thoroughly studied by Loew (née Harris), and Maltempo and Moss, who developed a useful theoretical framework for electronic structures with axial symmetry.[26] Given the markedly orthorhombic character of

 © 2006 Wiley-VCH Verlag GmbH & Co. KGaA, Weinheim

the electronic structure of the Fe^{III} center in **1**, a new model was needed to account for its magnetic properties. For this purpose, we have developed an ad hoc model that takes into consideration all the following interactions: interelectronic, spin–orbit, ligand-field, and Zeeman.[9]

The total number of possible states in a d^5 configuration is 252, but in accordance with previous results,[27] only the 18 states derived from the $^6A_1$ and $^4T_1$ cubic terms seem to be of major significance. Accordingly, we restricted our calculations to these states. In D_2 symmetry and in the absence of spin–orbit interactions, the orbital triplet $^4T_1$ splits into three singlets, namely $^4B_1$, $^4B_2$, and $^4B_3$, which transform as z, y, and x, respectively ($^4T_0$, ^4T_y, and ^4T_x). The interelectronic and ligand-field contributions are described by the parameters Δ_o, Δ_t, and δ, which are defined as the energy differences between the appropriate terms (Figure 3).

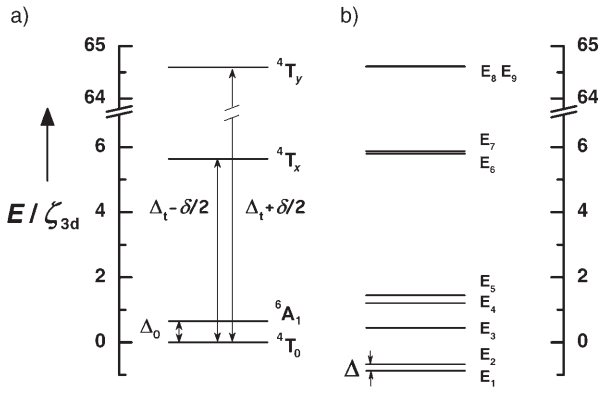

Figure 3. Energy diagrams of the relevant levels of **1** in D_2 symmetry. a) Terms in the absence of spin–orbit coupling; ordering depends on the actual value of Δ_o, Δ_t, and δ, which are defined in the text. b) Structure of the Kramers doublets after inclusion of the spin–orbit interaction.

Introduction of the spin–orbit interaction with a ζ_{3d} monoelectronic coupling coefficient gives a set of nine Kramers doublets (Figure 3). The base function of each of these doublets is obtained as a linear combination of the uncoupled $^4T_1$ and $^6A_1$ wave functions.[9] The coefficients of these linear combinations depend only on the dimensionless parameters u, v, and w, which are related to the aforementioned Δ_o, Δ_t, δ parameters by the expressions in Equation (1).

$$u = \frac{\Delta_t}{\zeta_{3d}}, \quad v = \frac{\delta}{\Delta_t} = \frac{\delta}{\zeta_{3d}}\frac{1}{u}, \quad w = \frac{\Delta_o}{\zeta_{3d}} \tag{1}$$

At a sufficiently low temperature, only the lowest Kramers doublet would be populated. Accordingly, the EPR spectrum of **1** can be assigned to transitions between the states originating from that level by Zeeman interaction. Following our model, the principal effective g values of this $S' = {}^1/_2$ entity depend only on the parameters u, v, and w. An estimate of these coefficients can therefore be made by fitting the calculated g'_x, g'_y, and g'_z values to the experimentally observed ones. The best fitting yields the values $u = 35.1(2.7)$, $v = 1.68(3)$, and $w = 0.65(4)$, which allow us to calculate the energies (Figure 3) and the wave functions (see Supporting Information) of all nine levels involved.[9] For the ground state (E_1) and the first excited state (E_2) the $S = {}^3/_2$ contribution is about 64 %.

Taking into account that ζ_{3d} is approximately 420 cm^{-1} for the free Fe^{III} ion, and considering the energy diagram depicted in Figure 3, only the two lowest-lying energy doublets (E_1 and E_2) need to be considered when calculating the thermal dependence of the magnetic moment, $\mu(T)$ [Eq. (2)].

$$\mu(T) = \mu_B\left[C_1 + C_2\left(\frac{2k_BT}{\Delta}\right)\tanh\left(\frac{\Delta}{2k_BT}\right) + C_3\tanh\left(\frac{\Delta}{2k_BT}\right)\right]^{1/2} \tag{2}$$

The dimensionless coefficients C_1, C_2, and C_3 depend only on the parameters u, v, and w; Δ is the energy difference between the E_1 and E_2 levels (Figure 3). Since the values of C_1, C_2, and C_3 are determined by the EPR data, the magnitude of Δ can be estimated by fitting the expression given in Equation (2) to the experimentally observed $\mu(T)$. The best fitting for the whole thermal evolution (solid line in Figure 2c) is obtained with $\Delta = 78(3)$ cm^{-1}, which yields the calculated μ_0 and μ_∞ values given in Table 1. On the other hand, $\Delta/\zeta_{3d} = 0.20$, as deduced from the u, v, and w values. This means that ζ_{3d} is 390(15) cm^{-1} in our compound, which is a slight decrease with respect to the free ion value, as commonly found in transition-metal chemistry. In addition, the unpaired electronic distribution in the two levels E_1 and E_2 is practically indistinguishable (see Supporting Information), which explains why the quadrupolar splitting is unaffected by temperature. On the other hand, the thermal averaging of E_1 and E_2 with increasing temperature should involve averaging of the "third component" of the spin and orbital moments. This could result in a drastic reduction of the hyperfine coupling and therefore in a narrowing of the Mössbauer quadrupolar lines,[28] as observed experimentally (see Supporting Information and Figure 2a). The thermal dependence of the EPR spectrum noted above, as well as the deviation observed in the g'_z value (Table 1), could also be due to this dynamic process, a detailed study of which is beyond the scope of the present communication. Otherwise, a remarkably good agreement between calculated and experimental values for the relevant parameters, associated with the magnetic properties of **1** (Table 1), is provided by our ad hoc model.

To summarize, the magnetic properties of the SP-4 compound $[Li(thf)_4][Fe^{III}(C_6Cl_5)_4]$ (**1**) reveal that the Fe^{III} center behaves as a spin-admixed species ($S = {}^3/_2, {}^5/_2$). Thus, even in the absence of axial ligands, the sextet state may be sufficiently close in energy to the quartet ground state to enable a significant admixture with it.

Received: May 5, 2006
Published online: September 15, 2006

Keywords: EPR spectroscopy · homoleptic compounds · iron · magnetic properties · Moessbauer spectroscopy

 © 2006 Wiley-VCH Verlag GmbH & Co. KGaA, Weinheim

[1] *Chemistry of Iron* (Ed.: J. Silver), Blackie Academic & Professional, Glasgow, UK, **1993**.

[2] *Metal Sites in Proteins and Models: Iron Centres* (Eds.: H. A. O. Hill, P. J. Sadler, A. J. Thomson), Springer, Berlin, **1999**.

[3] "Bioinorganic Chemistry": A. X. Trautwein, E. Bill, E. L. Bominaar, H. Winkler, *Struct. Bonding (Berlin)* **1991**, *78*, 1.

[4] S. Alvarez, J. Cirera, *Angew. Chem.* **2006**, *118*, 3078; *Angew. Chem. Int. Ed.* **2006**, *45*, 3012.

[5] F. A. Cotton, G. Wilkinson, C. A. Murillo, M. Bochman, *Advanced Inorganic Chemistry*, 6th ed., Wiley, New York, **1999**, chap. 17, Section E, pp. 775–814.

[6] "Spin Crossover in Transition Metal Compounds I": P. J. van Koningsbruggen, Y. Maeda, H. Oshio, *Top. Curr. Chem.* **2004**, *233*, 259.

[7] W. R. Scheidt, M. Gouterman in *Iron Porphyrins*, *Part I* (Eds.: A. B. P. Lever, H. B. Gray), Addison–Wesley, Reading, MA, **1983**, chap. 2, pp. 89–139; W. R. Scheidt, C. A. Reed, *Chem. Rev.* **1981**, *81*, 543.

[8] R. L. Carlin, *Science* **1985**, *227*, 1291.

[9] A more detailed description can be found in the Supporting Information.

[10] R. Nast, F. Urban, *Z. Anorg. Allg. Chem.* **1956**, *287*, 17.

[11] R. B. Kerber in *Comprehensive Organometallic Chemistry II*, *Vol. 7* (Eds.: E. W. Abel, F. G. A. Stone, G. Wilkinson, D. F. Shriver, M. I. Bruce), Elsevier, Oxford, UK, **1995**, chap. 2, pp. 101–229; M. D. Johnson in *Comprehensive Organometallic Chemistry*, *Vol. 4* (Eds.: G. Wilkinson, F. G. A. Stone, E. W. Abel), Pergamon, Oxford, UK, **1982**, Section 31.2, pp. 331–376.

[12] A. Fürstner, H. Krause, C. W. Lehmann, *Angew. Chem.* **2006**, *118*, 454; *Angew. Chem. Int. Ed.* **2006**, *45*, 440; H. J. Spiegl, G. Groh, H. J. Berthold, *Z. Anorg. Allg. Chem.* **1973**, *398*, 225.

[13] C. Bolm, J. Legros, J. Le Paih, L. Zani, *Chem. Rev.* **2004**, *104*, 6217; J. K. Kochi, *J. Organomet. Chem.* **2002**, *653*, 11.

[14] G. Champetier, *Bull. Soc. Chim. Fr.* **1930**, *47*, 1131. For a detailed account of early results, see: F. A. Cotton, *Chem. Rev.* **1955**, *55*, 551.

[15] T. J. Kealy, P. L. Pauson, *Nature* **1951**, *168*, 1039.

[16] B. K. Bower, H. G. Tennent, *J. Am. Chem. Soc.* **1972**, *94*, 2512.

[17] P. J. Alonso, J. Forniés, M. A. García-Monforte, A. Martín, B. Menjón, C. Rillo, *Chem. Eur. J.* **2002**, *8*, 4056; P. J. Alonso, L. R. Falvello, J. Forniés, M. A. García-Monforte, A. Martín, B. Menjón, G. Rodríguez, *Chem. Commun.* **1998**, 1721.

[18] J. Cirera, P. Alemany, S. Alvarez, *Chem. Eur. J.* **2004**, *10*, 190.

[19] D. Jacoby, C. Floriani, A. Chiesi-Villa, C. Rizzoli, *J. Chem. Soc. Chem. Commun.* **1991**, 220.

[20] D. Bhattacharya, S. Dey, S. Maji, K. Pal, S. Sarkar, *Inorg. Chem.* **2005**, *44*, 7699.

[21] C. A. Reed, F. Guiset, *J. Am. Chem. Soc.* **1996**, *118*, 3281.

[22] Considering the different single-bond covalent radii of carbon (77 pm) and nitrogen (70 pm), the average Fe^{III}–C bond length in **1** (206 pm) is comparable to the average Fe^{III}–N distance (ca. 198 pm) in five-coordinate tetraphenylporphyrin (tpp) complexes of the type $[Fe^{III}(tpp)X]^-$, where X is a weakly coordinating ligand. Moreover, the small tetrahedral distortion discussed above for the anion $[Fe^{III}(C_6Cl_5)_4]^-$, as well as the helicoidal arrangement of the four aryl rings, can be related to the saddling (*sad*, B_{2u})- and propelling (*pro*, A_{1u})-type normal deformations of metalloporphyrins respectively: W. Jentzen, X.-Z. Song, J. A. Shelnutt, *J. Phys. Chem. B* **1997**, *101*, 1684.

[23] The Mössbauer spectra of **1** typically contain variable amounts of a minor species with the following spectral parameters: $\delta = 0.47(1)\ mm\,s^{-1}$ and $\Delta E_Q = 0.68(1)\ mm\,s^{-1}$. These parameters are attributable to a high-spin Fe^{III} by-product formed by thermal degradation and aging of **1** both in solution and in the solid state. The contribution of this by-product to the total signal in the spectrum in Figure 2a is less than 5%.

[24] H. Keutel, I. Käpplinger, E.-G. Jäger, M. Grodzicki, V. Schünemann, A. X. Trautwein, *Inorg. Chem.* **1999**, *38*, 2320.

[25] χ_{TI} was estimated from the temperature dependence of the χT product at high temperature. The contribution of the minor by-product detected by Mössbauer spectroscopy was also taken into account.[23]

[26] G. H. Loew in *Iron Porphyrins*, *Part I* (Eds.: A. B. P. Lever, H. B. Gray), Addison–Wesley, Reading, MA, **1983**, chap. 1, pp. 1–87; M. M. Maltempo, T. H. Moss, *Q. Rev. Biophys.* **1976**, *9*, 181; G. Harris, *Theor. Chim. Acta* **1968**, *10*, 155; G. Harris, *Theor. Chim. Acta* **1968**, *10*, 119.

[27] X.-Y. Kuang, I. Morgenstern-Badarau, *Phys. Status Solidi B* **1995**, *191*, 395.

[28] E. Bradford, W. Marshall, *Proc. Phys. Soc. London* **1966**, *87*, 731.

 © 2006 Wiley-VCH Verlag GmbH & Co. KGaA, Weinheim